Chemical Science

Accepted Manuscript

This article can be cited before page numbers have been issued, to do this please use: H. Ogawa, L. Yu, S. Li, Y. Nagata, T. K. Chan, Y. Matsuda, J. Liu, Y. Li and H. Nakamura, *Chem. Sci.*, 2026, DOI: 10.1039/D6SC03088B.

ROYAL SOCIETY OF CHEMISTRY

rsc.li/chemical-science

View Article Online
DOI: 10.1039/D6SC03088B

ARTICLE

Reprogramming RiPP Scaffolds through Skeletal Editing Unlocks Chemical Space

Received 00th January 20xx,
Accepted 00th January 20xx

DOI: 10.1039/x0xx00000x

Hiroshige Ogawa, [†a] Longhui Yu, [†a] Shangzhao Li, [a] Yuuya Nagata, [b] Tsz Ki Chan, [c] Yudai Matsuda, [c] Jing Liu, [d] Yong-Xin Li, [d] Hugh Nakamura*[a]

In this study, we report (1) a scalable, systematic, and general synthetic approach for the supply of ribosomally synthesized and post-translationally modified peptides (RiPPs) bearing Tyr–Trp cross-linkages, and (2) the comprehensive expansion of novel chemical space through their skeletal diversification. In recent years, numerous biaryl-containing peptides have been discovered, and some of these RiPPs exhibit potent biological activities. However, despite the high metabolic stability and strong target protein binding generally attributed to biaryl RiPPs, their significant strain and rigidity have limited the availability of general synthetic methods. Here, we demonstrate the high versatility of modular synthetic strategies for the construction of RiPPs and achieve the synthesis of a variety of RiPPs containing Tyr–Trp cross-linkages. Furthermore, skeletal diversification via scaffold hopping enables access to artificial RiPP scaffolds incorporating quinazoline and quinoline motifs, whose preparation has previously been challenging.

Introduction

Advances in genome mining technologies, which enable the discovery of previously overlooked but potentially valuable genes from biological genomes, have led in recent years to the identification of numerous ribosomally synthesized and post-translationally modified peptides (RiPPs) that were not recognized before.[1–6] Because the core scaffolds of RiPPs can, to a large extent, be predicted from their genomic sequences, the number of newly reported RiPPs has been increasing at an explosive pace worldwide.[7–10] Among them are noncanonical cyclic peptides bearing rigid biaryl motifs embedded within their macrocyclic frameworks (Figure 1).[6,11–18] Compared with conventional cyclic peptides, these rigid cyclic peptides are characterized by enhanced stability in biological systems and reduced susceptibility to proteolytic degradation.[19–22] In addition, their conformational rigidity is considered to promote stronger binding to target proteins than that achieved by more flexible cyclic peptides, thereby conferring higher selectivity.[23–25] Some of these noncanonical cyclic peptides also exhibit potent biological activities, including antimicrobial properties.[26–34]

Despite their promise as attractive and potentially valuable drug discovery seeds, general and scalable synthetic routes to such rigid peptides remain limited to date.[9,12,14,35–38] For example, enzymatic production often affords only several to several tens of milligrams of the final products, which is disadvantageous in terms of scalability and the preparation of analogues for further activity optimization.[9,12,35,37,38] In the case of purely chemical synthesis, conventional macrocyclization methods are frequently not applicable to these rigid noncanonical cyclic peptides.[39–43] For instance, it has been shown that the Trp $N1$-to-Trp $C7'$ cross-linkage present in cihunamide B (**1**)[44] and strecintide 839 (**2**)[45] cannot be constructed by classical intramolecular (or intermolecular) Ullmann couplings using CuI, which represent a standard approach to biaryl macrocyclization. Likewise, the Tyr $C6$-to-Trp $N1'$ cross-linkage found in lapparbin (**3**)[46] is not accessible via intramolecular Ullmann coupling. Furthermore, the highly strained cyclic framework of micitide 982 (**5**), which contains a Tyr $C6$-to-Trp $C5'$ cross-linkage, has been shown to be inaccessible by conventional macrocyclization using standard amide coupling reagents such as HATU, EDCI, PyBOP, or COMU.[47] Thus, even though medium-sized molecules are attracting increased attention as a new modality in drug discovery and the importance of cyclic peptides has been growing, robust, scalable, and generally applicable synthetic methods for these rigid noncanonical cyclic peptides—particularly those that enable systematic analog synthesis—have yet to be established.

Conventional synthetic approaches to cyclic peptides bearing biaryl architectures are illustrated in Figure 2A. Among the most reliable methods for achieving sp^2–sp^2 coupling, Suzuki–Miyaura[48–50] and Stille couplings[51] represent highly effective reactions for constructing biaryl linkages. However, these strategies require prior, separate functionalization of both aromatic rings (*e.g.*, halogenation, borylation, or stannylation). This prerequisite limits the modularity of the synthesis, as diverse biaryl motifs cannot be introduced at late stages, rendering these methods unsuitable for analog generation. In contrast, oxidative coupling, which directly connects two aromatic rings without the need for prefunctionalization, offers practical advantages for the efficient synthesis of natural products and specific compounds.[36] Nevertheless, oxidative coupling is strongly dependent on the electronic density of the aromatic substrates, restricting its applicability to particular amino acid units

[a] The Hong Kong University of Science and Technology, Clear Water Bay, Hong Kong SAR, China. Email: hnakamura@ust.hk
[b] Autonomous Polymer Design and Discovery Group Research Center for Macromolecules and Biomaterials, National Institute for Materials Science (NIMS), 1-2-1 Sengen, Tsukuba, Ibaraki, 305-0047, Japan
[c] City University of Hong Kong, Tat Chee Avenue, Kowloon, Hong Kong SAR, China
[d] Department of Chemistry and The Swire Institute of Marine Science, The University of Hong Kong, Hong Kong SAR, China
† Contributed equally.

View Article Online
DOI: 10.1039/D6SC03088B

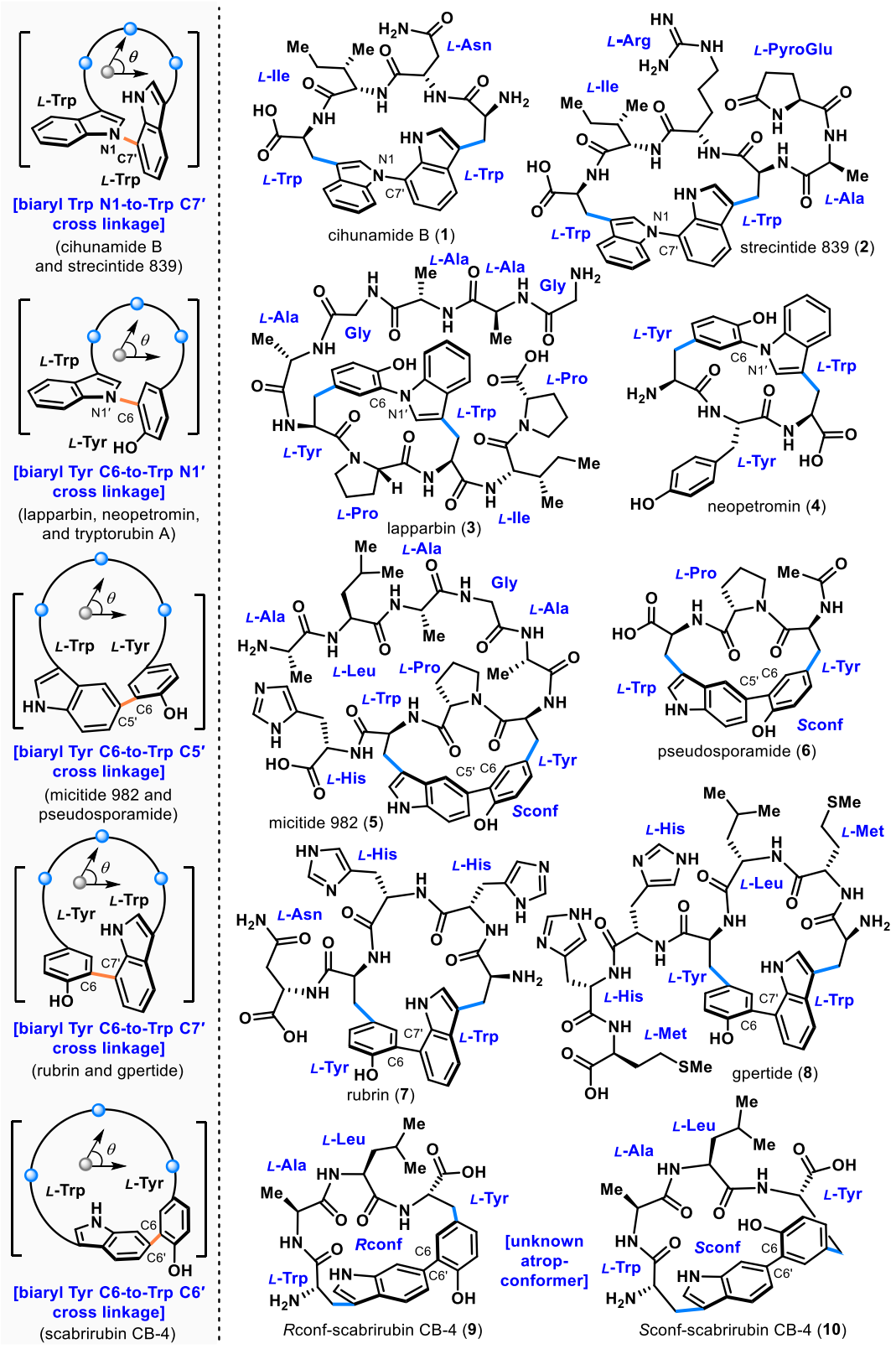

Fig. 1 Representative noncanonical biaryl cyclic peptides.

View Article Online
DOI: 10.1039/D6SC03088B

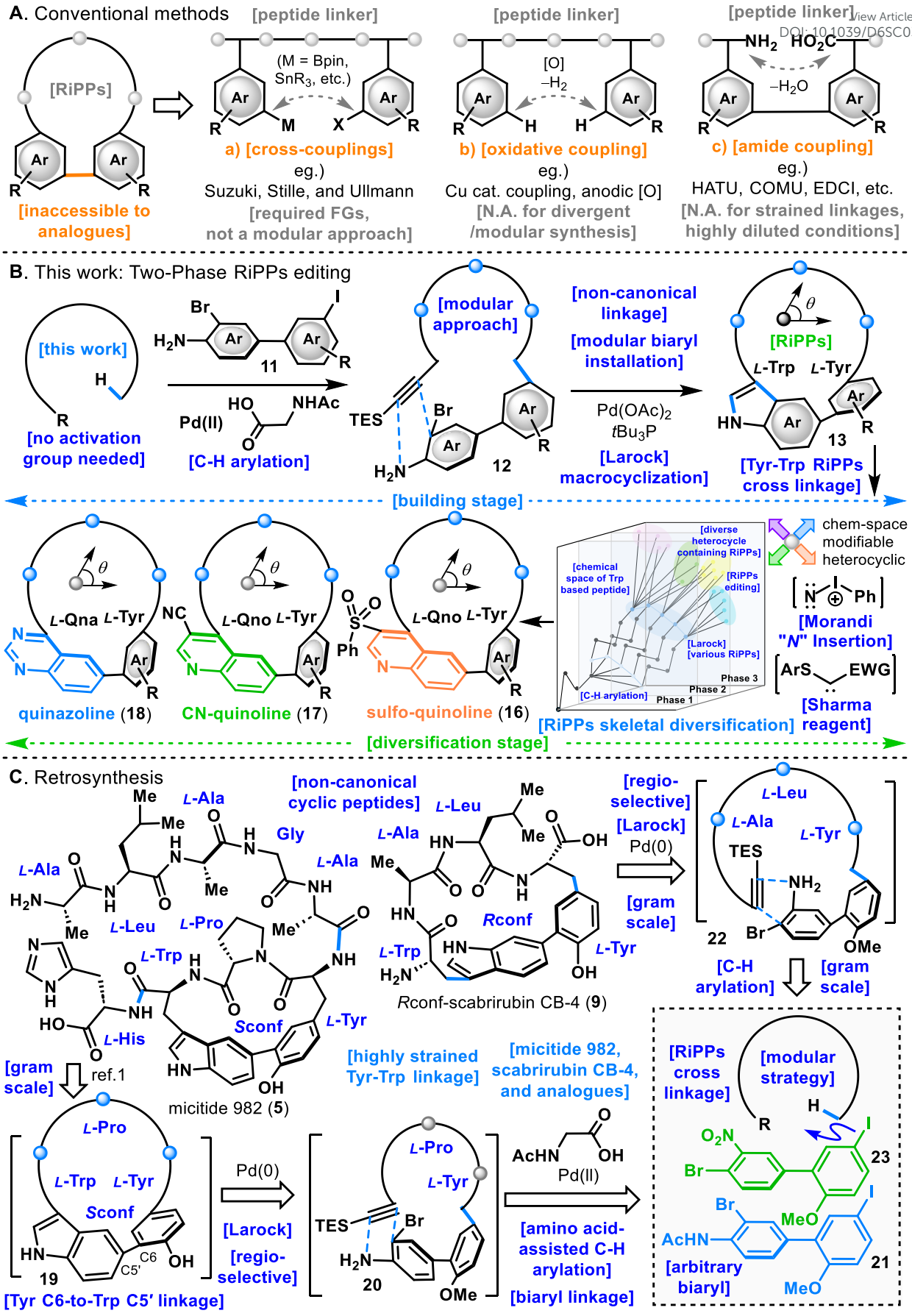

Fig 2. Conventional methods to construct RiPPs and the concept of this work

and thereby limiting its utility in analog synthesis. Furthermore, the inability to freely introduce biaryl units at advanced stages of synthesis reduces the modularity of this approach. Intramolecular amide bond formation for macrocyclization has long been one of the most representative methods for cyclic peptide synthesis.[39–43] However, when rigid, linear biaryl units are present in the substrate, the associated strain may prevent intramolecular amide coupling from proceeding.[47,52,53] Even when macrocyclization is successful, extremely dilute conditions are often required, posing challenges for analog synthesis and scalability.

Beyond these established strategies, there exists a chemical space comprising molecular entities that are theoretically accessible but remain practically restricted due to the lack of generalized synthetic routes.[32,54–66] Some of these molecular assemblies may exhibit biological activities or mechanisms of action distinct from known natural products or pharmaceuticals, potentially contributing to novel therapeutic modalities. In recent years, global efforts have focused on developing new molecular transformation strategies, including skeletal editing and scaffold rearrangements, to efficiently access such chemical space.[67–80] Expansion of this space has enabled entry into molecular classes that were previously difficult to synthesize.

Our group has recently contributed to the development of general, modular synthetic methods for rigid noncanonical cyclic peptides, exemplified by RiPPs such as cihunamide B (**1**)[44], strecintide 839 (**2**)[45], lapparbin (**3**)[46], neopetromin (**4**)[81], and micitide 982 (**5**)[47]. These methods allow gram-scale supply of noncanonical cyclic peptides but rely on Larock macrocyclization, which has limited applicability to natural scaffolds, particularly beyond indole-derived frameworks. To overcome this limitation, we envisioned a two-phase strategy: in the first stage, biaryl-containing RiPP scaffolds would be assembled using a modular and scalable approach; in the second stage, skeletal diversification would be applied to edit the indole framework, thereby granting access to previously inaccessible regions of chemical space (Figure 2B).

As demonstrated in our recent synthesis of lapparbin (**3**)[46], biaryl motifs can be introduced into amino acid units via C–H arylation, followed by Pd(0)-catalyzed Larock macrocyclization to generate Tyr–Trp RiPP cross-linkages at an early stage. Subsequent application of skeletal diversification strategies, such as those recently reported by Morandi[82–84] and Sharma[85,86] for the synthesis of quinazolines and quinolines, is expected to expand RiPP chemical space into previously inaccessible domains. The hallmark of this approach lies in the early-stage construction of RiPP scaffolds using modular, scalable methods, followed by skeletal diversification to furnish diverse quinazoline and quinoline derivatives from common intermediates, thereby broadening chemical space.

Guided by this concept, we targeted micitide 982 (**5**)[18] and scabrirubin CB-4 (**9, 10**)[14], both Tyr–Trp cross-linked RiPPs, for chemical space expansion through a two-phase sequence combining C–H arylation and skeletal diversification (Figure 2C). Scabrirubin CB-4 (**9**, **10**) is a non-natural atropo-peptide recently generated by combinatorial biosynthesis.[14] Its atropisomeric configuration has not yet been reported. In this study, we planned the synthesis of scabrirubin CB-4 (**9**, **10**) to determine its atropisomeric arrangement. Scabrirubin CB-4 (**9**, **10**) was expected to arise from cyclization precursor **22** via regioselective Larock macrocyclization. Precursor **22** would be prepared by introducing biaryl derivative **23** into an amino acid unit through carboxylic acid-directed C–H arylation. A key advantage of this synthetic strategy is its modularity, enabling comprehensive access to RiPPs bearing diverse biaryl units through analogous approaches. For example, micitide 982 (**5**) was planned to be synthesized from biaryl derivative **21**, introduced into an amino acid unit via carboxylic acid-directed C–H arylation, to furnish precursor **20**. Precursor **20** would then undergo regioselective Larock macrocyclization, followed by side-chain elaboration, to yield micitide 982 (**5**). Furthermore, both scabrirubin CB-4 (**9**, **10**) and micitide 982 (**5**) are expected to serve as platforms for skeletal diversification, enabling expansion into RiPP derivatives bearing quinazoline or quinoline frameworks—chemical spaces that have previously been difficult to access. Overall, this synthetic strategy represents a versatile, modular supply method applicable not only to scabrirubin CB-4 (**9**, **10**) and micitide 982 (**5**) but also to a wide range of RiPPs.

Results and Discussion

The total synthesis of micitide 982 (**5**) commenced with the C–H arylation of biaryl unit **21** and alanine derivative **24** (Scheme 1). Our group has recently reported an electrochemical approach to the synthesis of micitide 982 (**5**).[47] In that method, C–C bond formation between a serine-derived alkyl bromide and a biaryl unit required Ni-catalysis, necessitating prior activation of the serine alcohol moiety through conversion into the corresponding alkyl bromide derivative. However, introduction of the biaryl fragment into the amino acid unit via Ni-catalyzed electrochemical C–C bond formation was hampered by competing side reactions such as reduction, elimination, and dimerization of the alkyl bromide precursor, limiting the yield to a maximum of 47%.

By contrast, C–H arylation provides a direct means of introducing aromatic units into amino acid residues without the need for prior activation. Numerous C–H arylation reactions have been reported.[87–94] However, many of these methods require a directing group at the *C*–terminus, typically an aminoquinoline.[95–107] For application to total synthesis, removal of the directing group is required, which entails multistep manipulations and suffers from low overall yields.[104,106,108–112] Initially, C–H activation of an *N*–phthaloyl alanine derivative bearing an aminoquinoline at the C–terminus with biaryl **23** was attempted. Although the C–H activation proceeded in good yield, subsequent protecting-group manipulation required three steps, and the overall yield was not satisfactory (25%), highlighting the limited practicality of this approach (see Supporting Information). Thus, the development of a more practical methodology was essential.

More recently, carboxylic acid-free C–H arylations of amino acids that do not require aminoquinoline ligands have been developed.[95] The advantages of these methods include not only the direct incorporation of aromatic fragments into amino acids but also the avoidance of side reactions (reduction, elimination, dimerization) associated with the use of serine-derived alkyl bromides.[47] Based on this rationale, a direct C–H arylation strategy was adopted to introduce biaryl unit **21** into commercially available alanine derivative **24**. This transformation proceeded efficiently using glycine derivative **25** as a ligand, affording compound **26** in 71% yield on a gram scale.

Compound **26** was subsequently converted into carboxylic acid **27** by removal of the phthalimide group with ethylenediamine, followed by Boc protection. Sequential condensation of proline derivative **28** and alkyne fragment **30** with **27** using HATU furnished cyclization precursor **31**. Regioselective Larock macrocyclization[44,45,47,52,81,113–125] of precursor **31** under Pd(0) catalysis afforded cyclic compound **32** bearing a Tyr *C*6–to–Trp *C*5′ cross-linkage. Removal of the TES group from **32** yielded compound **33**, possessing the RiPP scaffold.

Scheme 1[a] Total synthesis of micitide 982 (5) and its skeletal diversification.

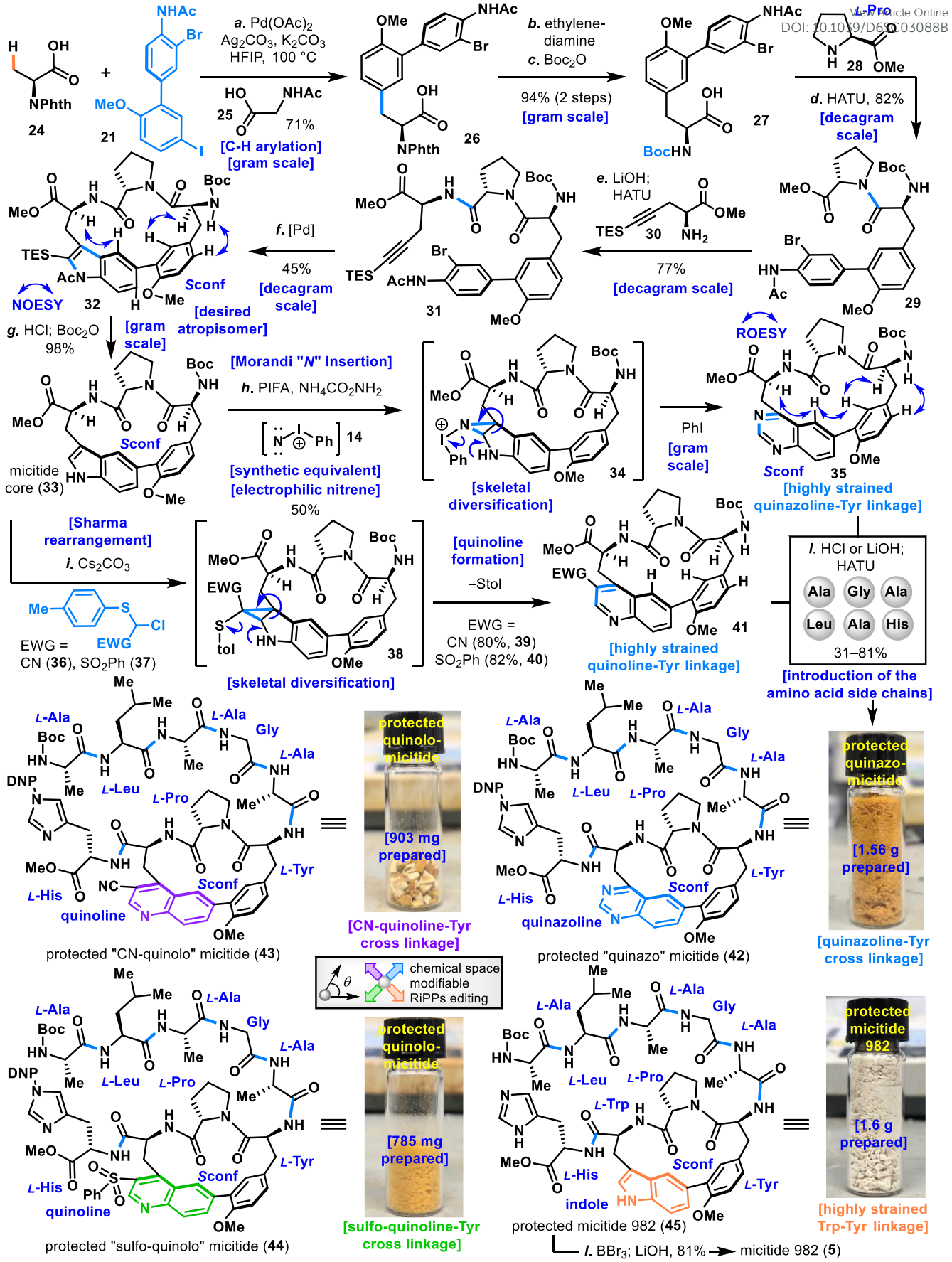

[a]For detailed reagents and conditions, see the Supporting Information.

Next, skeletal diversification was employed to expand the chemical space of RiPP scaffold **33** toward quinazoline and quinoline derivatives. Morandi and co-workers recently reported a nitrene-mediated scaffold hopping of indoles to quinazoline derivatives.[82–84] In this transformation, the high nucleophilicity of the indole and the strong electrophilicity of the nitrene facilitate aziridine formation at the *C*2 and *C*3 positions, followed by ring opening to effect scaffold hopping and generate quinazoline derivatives.

Conversion of the indole moiety of tryptophan residues within peptides to a quinazoline scaffold is attractive from a drug-discovery perspective.[82–84] This transformation retains the indole's planar topology and hydrophobic interactions while markedly altering its hydrogen-bonding pattern. The quinazoline core replaces the indole's hydrogen-bond donor with two hydrogen-bond acceptors, and such skeletal editing of tryptophan is expected to modulate a compound's target selectivity and pharmacokinetic properties.[82–84] Moreover, tryptophan is prone to oxidation, which can reduce bioavailability and complicate formulation processes.[126,127] Skeletal editing to a quinazoline therefore has the potential to enhance oxidative resistance and address these issues. Application of this method to RiPP scaffold **33** was expected to enable access to quinazoline-containing RiPPs, which had previously been difficult to obtain due to strain. In parallel, Sharma and co-workers demonstrated that carbene precursors bearing toluenethiol substituents are effective for indole scaffold hopping, enabling facile conversion to quinoline derivatives.[85] Quinoline, like quinazoline, alters the hydrogen-bonding pattern of tryptophan and is expected to enhance metabolic stability.

These strategies were evaluated for RiPP scaffold **33**. Nitrene precursor **14** was generated *in situ* using PIFA and ammonium carbamate, effecting "*N*" insertion into scaffold **33**. The scaffold hopping proceeded smoothly, affording quinazoline derivative **35** bearing a Tyr cross-linkage via intermediate **34** in 50% yield. ROESY analysis and DFT calculations revealed that compound **35** possesses an *S*–configured atropisomeric axis. Notably, the atropisomeric axis of scaffold **33** was retained after "*N*" insertion. To date, scaffold hopping has not been applied to biaryl cyclic peptides. Thus, this study demonstrates that skeletal diversification enables late-stage, scalable, and efficient conversion of rigid biaryl cyclic peptides into artificial analogs with potentially distinct physical properties and biological activities.

Carbene-mediated ring expansion of RiPP scaffold **33** was also investigated. Using carbene precursors **36** and **37**, bearing toluenethiol and electron-withdrawing substituents, scaffold hopping of **33** was successfully achieved. The reaction proceeded efficiently via intermediate **38** to furnish quinoline derivatives **39** and **40**, each containing a Tyr cross- linkage, in good yields. Substituents such as –CN and $–SO_2Ph$ were successfully incorporated into the quinoline framework. These results demonstrate that scaffold hopping of RiPP scaffold **33** proceeds rapidly, enabling facile access to quinazoline derivative **35** and quinoline derivatives **39** (–CN) and **40** ($–SO_2Ph$) from a common indole precursor.

The synthesized RiPP scaffold **33**, quinazoline derivative **35**, and quinoline derivatives **39** (–CN) and **40** ($–SO_2Ph$) were each elaborated by sequential introduction of amino acid side chains to yield micitide 982 (**5**), protected "quinazo" micitide (**42**), protected "CN-quinolo" micitide (**43**), and protected "sulfo-quinolo" micitide (**44**). The modular construction of RiPP scaffolds via C–H arylation, followed by scaffold hopping, enabled the efficient and scalable generation of artificial RiPPs containing quinazoline and quinoline motifs from a single intermediate—an achievement of particular significance given the prior inaccessibility of such structures.

Finally, expansion of RiPP chemical space was pursued with scabrirubin CB-4 (**9** or **10**).[14] As noted above, scabrirubin CB-4 is a non-natural atropopeptide generated by combinatorial biosynthesis, and its atropisomeric configuration has not yet been reported. Accordingly, construction of the RiPP scaffold by C–H arylation and Larock macrocyclization, followed by scaffold hopping, was applied to scabrirubin CB-4 (Scheme 2). In analogy to the synthesis of micitide 982 (**5**), coupling of biaryl unit **23** with alanine derivative **24** via C–H arylation introduced the aromatic fragment into the amino acid residue, affording compound **46**. Compound **46** was then converted into amine **47** by methyl esterification of the carboxylic acid, followed by phthalimide removal.

Sequential condensation of amine **47** with leucine derivative **48** and alanine derivative **50** using HATU furnished compound **51**. The synthesized compound **51** was then subjected to amide coupling with alkyne fragment **30** to furnish macrocyclization precursor **52** on a gram scale. After reduction of the nitro group to the corresponding aniline, a Pd(0)-catalyzed regioselective Larock macrocyclization was attempted. Optimization revealed that the Larock macrocyclization proceeded efficiently to afford intermediate **53** and, subsequently, the protected scabrirubin CB-4 (**54**), a RiPP bearing a Tyr *C*6–to–Trp *C*6′ cross-linkage. Notably, this route proved amenable to scale-up, delivering 5.8 g of protected scabrirubin CB-4 (**54**). Global deprotection of **54** using BBr_3 followed by LiOH afforded, for the first time, scabrirubin CB-4 (**9**), an atropopeptide featuring a Tyr *C*6–to–Trp *C*6′ cross-linkage. The atropisomeric configuration of scabrirubin CB-4 (**9**) was assigned as *R* by ROESY analysis. Interestingly, although the HRMS data of synthetic R_{conf}–scabrirubin CB-4 (**9**) matched those reported for natural scabrirubin CB-4, the ^{1}H NMR spectra did not coincide.[14] Scabrirubin CB-4 (**55**) is biosynthesized from a ribosomally synthesized precursor peptide that undergoes post-translational modifications; therefore, the amino-acid backbone is expected to be in the L-configuration.[14,26] On this basis, we infer that the previously reported, configurationally unassigned scabrirubin CB-4 (**55**) likely corresponds to the opposite, *S* configuration.

To assess the thermodynamic stability of the cyclized product, protected scabrirubin CB-4 (**55**) was heated in toluene at 100 °C. No formation of *S*–conformation of scabrirubin CB-4 (**10**) was observed, suggesting that the synthetic *R*–conformation of scabrirubin CB-4 (**9**) is thermodynamically stable. Because the Larock indole synthesis requires prolonged heating at 110 °C, it is consistent that the synthetic scabrirubin CB-4 possesses a thermodynamically favored *R*–conformation. By contrast, the Tyr–Trp cross-link in the biosynthetic pathway is formed at room temperature, mediated by P450, which could lead to a different atropisomeric outcome. We next explored the expansion of chemical space via skeletal diversification of the obtained atropo-RiPP, *R*-conf-protected scabrirubin CB-4 (**55**). As a first step, the "*N*–insertion" strategy reported by Morandi and co-workers was applied.[82–84] Treatment of **55** with PIFA and $NH_4CO_2NH_2$ effected a smoothring-expansion, proceeding via intermediate **56**, to provide "quinazo"-scabrirubin CB-4 (**57**), a RiPP bearing a quinazoline–Tyr cross-linkage. In parallel, we examined the skeletal diversification of R_{conf}–protected scabrirubin CB-4 (**55**) using carbene precursors bearing a toluenethiol substituent, as described by Sharma and co-workers.[85] Sharma et al. have demonstrated that a variety of substituents (e.g., –CN, $–SO_2Ph$, $–PO(OEt)_2$) can be introduced via such carbene precursors. Accordingly, a series of carbene precursors was prepared and evaluated for scaffold hopping of the biaryl macrocycle **55**. This screening revealed that **55** could be converted into quinoline derivatives **59**–**61**, bearing –CN, $–SO_2Ph$, or $–PO(OEt)_2$ substituents, respectively. Of note, the skeletal diversification of R_{conf}–protected

View Article Online
DOI: 10.1039/D6SC03088B

Scheme 2[a]. Total synthesis of R_{conf}–scabrirubin CB-4 (9) and its skeletal diversification.

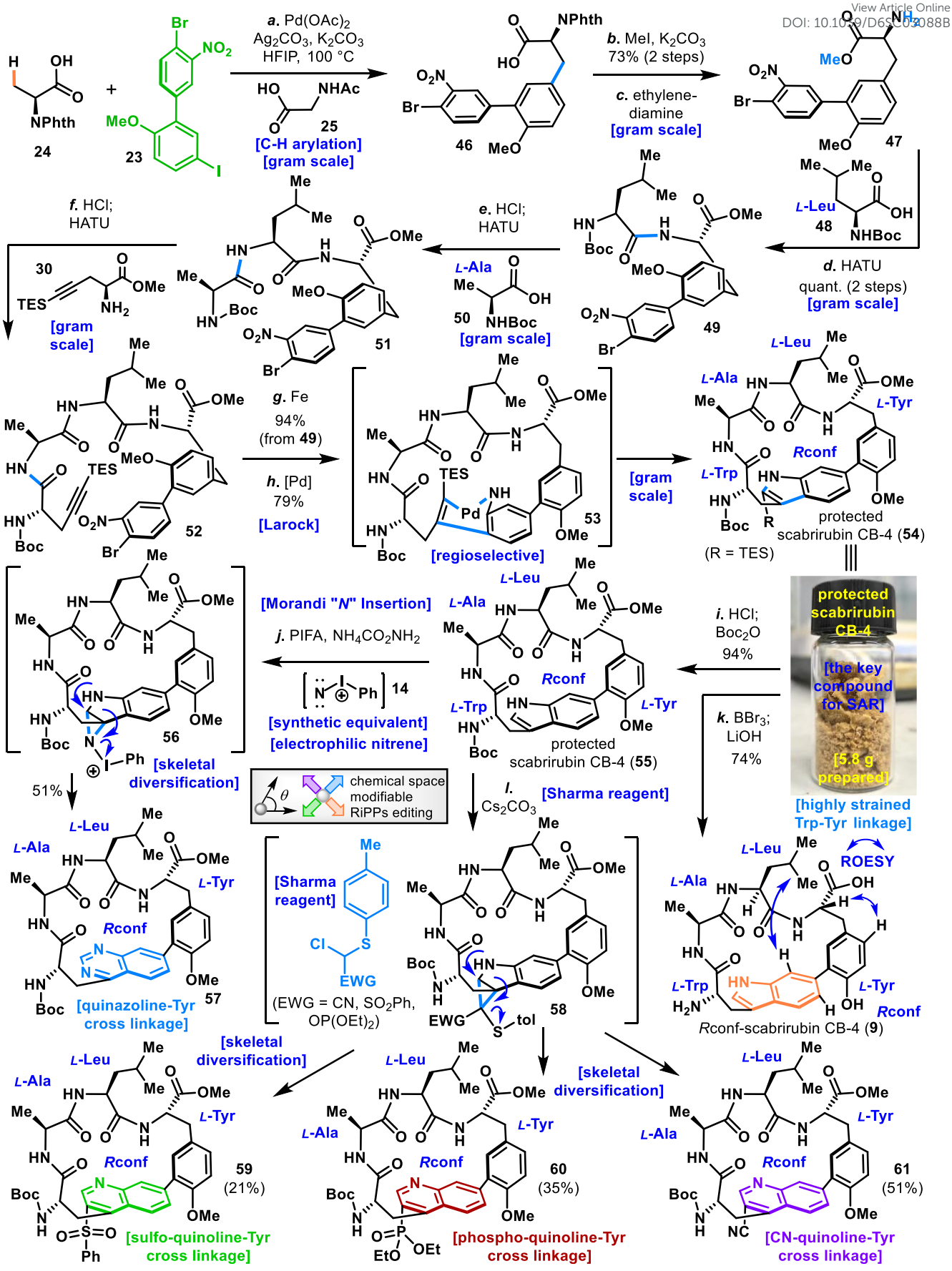

[a]For detailed reagents and conditions, see the Supporting Information.

View Article Online
DOI: 10.1039/D6SC03088B

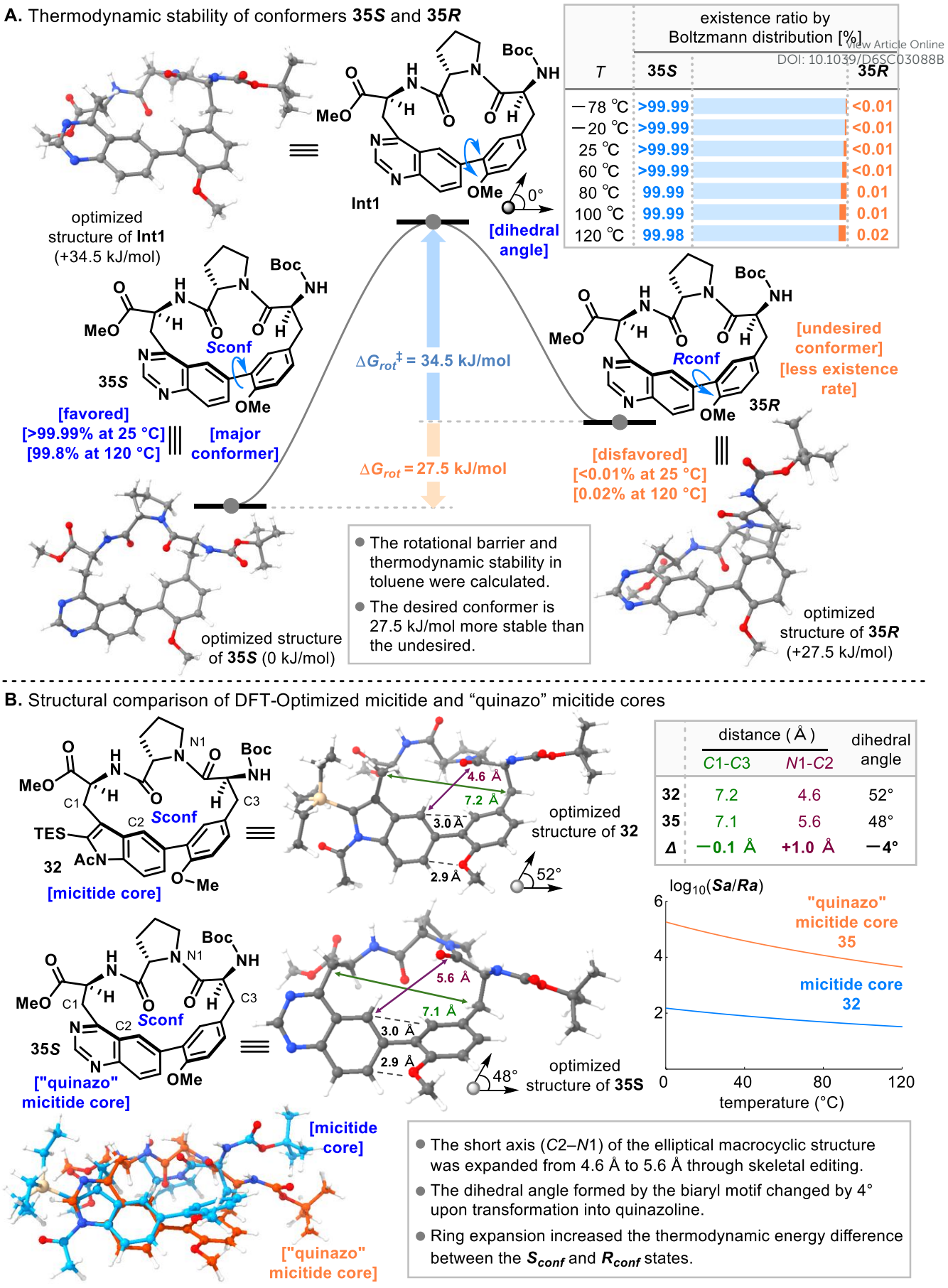

Fig. 3 DFT calculations on the thermodynamic stability of 35*S* and 35*R*.

scabrirubin CB-4 (**55**) proceeded in generally lower yields than the corresponding transformations of the micitide scaffold **33**. For example, the sulfo-quinoline–Tyr cross-linked product **59** was obtained in 21% isolated yield, whereas the phospho-quinoline–Tyr cross-linked analog **60** was isolated in 35% yield. This outcome can be rationalized by the higher intrinsic strain within R_{conf}–protected scabrirubin CB-4 (**55**), which likely slows the ring-expansion step from intermediate **58**. Indeed, species consistent with intermediate **58** were observed by TLC and MS analysis. Intermediate **58**, corresponding to sulfo-quinoline scabrirubin **59**, was isolated as an inseparable mixture of four stereoisomers by silica-gel chromatography. Treatment of this mixture with DIPEA in toluene at 100 °C induced ring-expansion to give compound **59**, albeit in low yield. In contrast, in the case of skeletal editing using micitide core **33**, no cyclopropane intermediate was detected by the LC-MS and TLC analysis with any of the carbene precursors employed. The ring expansion from the intermediate proceeded smoothly at room temperature. Consequently, yields for the overall skeletal editing process were relatively higher than the scabrirubin skeleton. These results suggest that the higher intrinsic strain of the scabrirubin framework impedes ring-expansion from intermediate **58**. The finding that the degree of macrocyclic strain in RiPPs can influence the rate of ring-expansion reactions is noteworthy and merits further attention.

The quinazoline–Tyr cross-linked product **35**, obtained by scaffold hopping of the RiPP micitide core **33**, was shown by ROESY to possess an *S*–configured chiral axis. It is particularly interesting that the atropisomeric configuration of the starting RiPP micitide scaffold **33** is preserved throughout the ring-expansion process to give quinazoline **35**. To gain further insight, the rotational barrier of the quinazoline–Tyr cross-linkage in **35** was investigated by DFT calculations (Figure 3). For the *S*– and *R*–atropisomers, **35*S*** and **35*R***, the calculated barrier for rotation from **35*S*** to **35*R*** was $\Delta G_{rot}^{\ddagger}$ = 34.5 kJ/mol. In general, atropisomers require a barrier of approximately 90 kJ/mol or higher to be separable at room temperature.[128] Thus, rotation about the chiral axis from **35*S*** to **35*R*** is, in principle, feasible at room temperature. However, comparison of the relative thermodynamic stabilities of **35*S*** and **35*R*** revealed that **35*R*** is higher in energy than **35*S*** by +27.5 kJ/mol. According to a Boltzmann distribution at 25 °C, this corresponds to a **35*S*/35*R*** ratio of >99.99:<0.01. Therefore, although rotation from **35*S*** to **35*R*** is theoretically possible at room temperature, the overwhelming thermodynamic preference for **35*S*** ensures that, in practice, **35*S*** is obtained in >99% abundance—consistent with experimental observations. Indeed, the single atropisomeric quinazoline **35** obtained by scaffold hopping was assigned as **35*S*** (*S*–configuration) by ROESY, and no trace of **35*R*** was detected experimentally. Furthermore, even at an elevated temperature of 120 °C, the Boltzmann distribution predicts a **35*S*/35*R*** ratio of 99.98:0.02, indicating that **35*S*** is highly stable and that its chiral axis is retained under high-temperature conditions.

To evaluate the effect of quinazoline incorporation on the molecular properties of RiPPs, a structural comparison was performed between the DFT-optimized micitide core **32**[47] and the "quinazo" micitide core **35** (Figure 3B). The major axis (*C*1–*C*3) of the elliptical macrocyclic structure differed by only 0.1 Å between the two cores, whereas the minor axis (*N*1–*C*2) was suggested to be 1.0 Å longer in the "quinazo" micitide core **35**. The dihedral angle was 52° in micitide core **32**, while in "quinazo" micitide core **35** it was 48°.

For the corresponding Larock macrocyclization product **32**, the rotational barrier between the *S*– and *R*–atropisomers was calculated to be $\Delta G_{rot}^{\ddagger}$ = 32.6 kJ/mol, comparable to that of **35** ($\Delta G_{rot}^{\ddagger}$ = 34.5 kJ/mol).[47] Intriguingly, DFT analysis showed that **32*S*** is more stable than **32*R*** by 11.4 kJ/mol. [47] This energy difference is substantially smaller than that between **35*S*** and **35*R*** (ΔG_{rot} = +27.5 kJ/mol). Thus, conversion of the indole unit to a quinazoline via scaffold hopping increases the energy gap between the *S* and *R* atropisomers, thereby enhancing the atropisomeric stability of the RiPP scaffold. Assuming a Boltzmann distribution, the relative populations of the S_{conf} and R_{conf} states were calculated from the thermodynamic energy differences obtained by DFT, and the common logarithm of the isomeric ratio, $\log_{10}(S_{conf}/R_{conf})$, was plotted as a function of temperature (Figure 3B). At all temperatures examined, the isomeric ratio of the "quinazo" micitide core was approximately 10^3-fold greater than that of the micitide core, indicating that the equilibrium is strongly shifted toward the S_{conf} state. For example, at 25 °C, the isomeric ratio of micitide core **32** was $S_{conf} : R_{conf}$ = 99 : 1, whereas that of the "quinazo" micitide core **35** was $S_{conf} : R_{conf} = 6.6 \times 10^4 : 1$, suggesting the strong shift of the equilibrium toward the S_{conf} state.

This effect is likely attributable to the replacement of the five-membered indole ring by a six-membered quinazoline moiety, which significantly alters the overall macrocyclic conformation. Upon superimposition of the DFT-optimized structures of micitide core **32** (sky blue, Figure 3B) and the 'quinazo' micitide core 35*S* (orange, Figure 3B), a pronounced alteration of the entire ring architecture is observed. Skeletal editing to introduce quinazoline induced not only local changes around the biaryl motif but also substantial alterations in the overall cyclic framework. This structural reorganization is presumed to have caused a pronounced shift in the equilibrium between the S_{conf} and R_{conf}.

To further validate the generality and utility of the modular synthesis of RiPP scaffolds based on C–H arylation and regioselective Larock macrocyclization, we examined a range of non-natural biaryl units (Figure 4A). In addition to biaryl motifs that can be elaborated into micitide 982 (**5**) and scabrirubin CB-4 (**9**) (compounds **26** and **46**), amino-acid-assisted C–H arylation was successfully applied to substrates in which the aromatic ring on the tyrosine side was substituted with a methyl group, affording the corresponding carboxylic acid **63**.

Introduction of RiPP scaffolds onto the obtained biaryl units was next investigated (Figure 4B). A key feature of this synthetic strategy is its ability to provide a variety of biaryl-containing RiPPs in a modular manner. Thus, carboxylic acid **63** was first coupled with proline derivative **28** using HATU, followed by attachment of alkyne fragment **30** to furnish the corresponding macrocyclization precursor. The macrocyclization proceeded efficiently in the presence of Pd(0) and a bulky ligand, affording the micitide 982 analogue **68**, bearing a Trp–4Me–Phe cross-linkage, on a 1.31 g scale. Likewise, application of the same modular sequence to carboxylic acid **64** provided RiPP scaffold **69**, featuring a Trp–Phe cross-linkage, on an 897 mg scale. Fluorinated, electron-deficient RiPP scaffolds are expected to exhibit increased oxidative stability and enhanced metabolic stability in biological systems.[129–131] Accordingly, macrocyclization of carboxylic acids **66** and **65** was examined under analogous conditions. The modular sequence again proceeded smoothly to afford fluorinated artificial RiPPs **70** and **71**, bearing Trp–3F–Phe and Trp–4F–Phe cross-linkages, respectively. Collectively, these results demonstrate that a broad range of biaryl motifs can be incorporated into RiPP frameworks using the present modular strategy based on C–H arylation and Larock macrocyclization. Systematic expansion of chemical space via skeletal diversification of the resulting RiPP scaffolds was then pursued to evaluate the generality of this approach (Figure 5). Carbene precursors bearing various substituents

View Article Online DOI: 10.1039/D6SC03088B

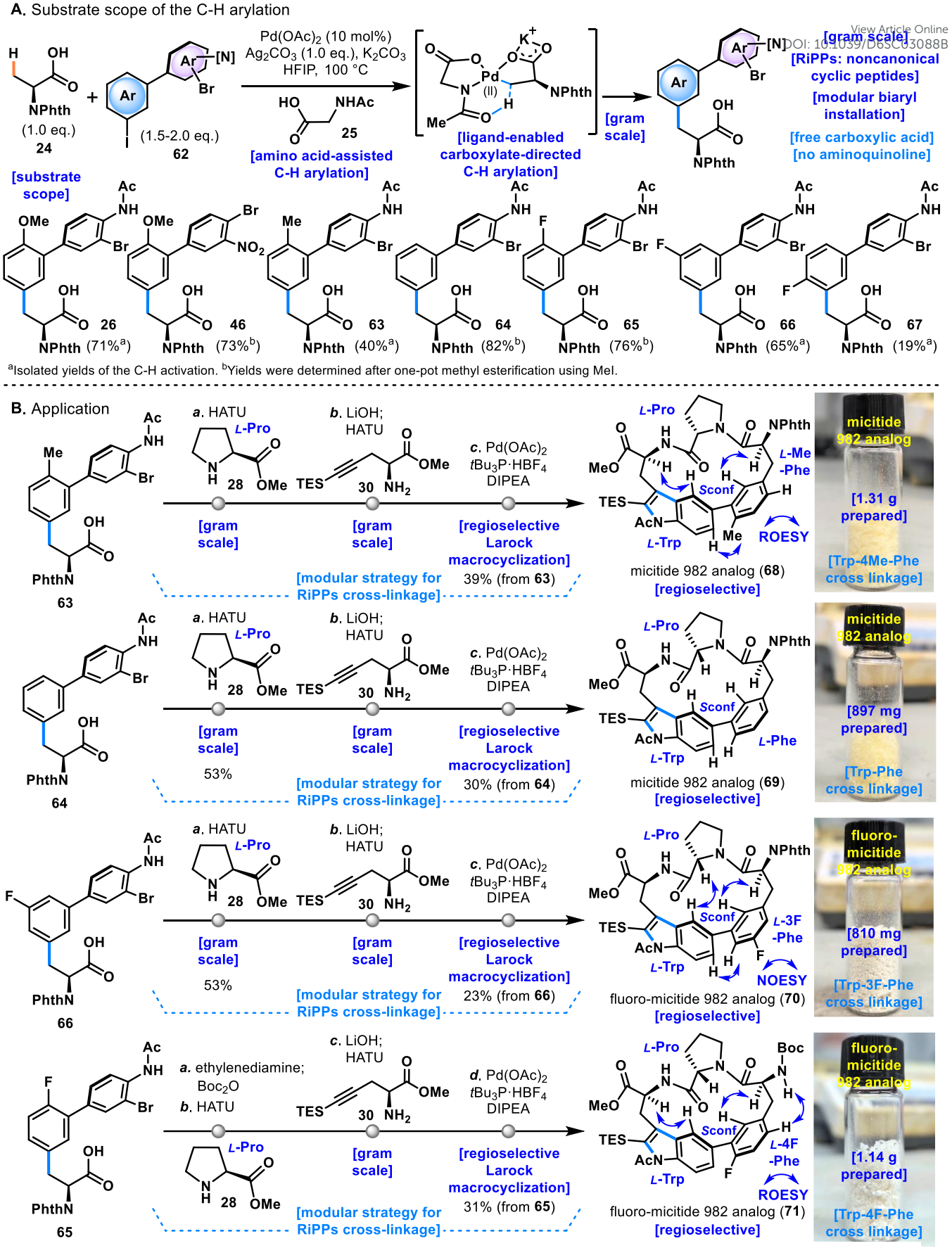

Fig. 4[a] Modular synthesis of RiPP scaffolds based on C-H arylation and Larock cyclization.
[a]For detailed reagents and conditions, see the Supporting Information.

View Article Online
DOI: 10.1039/D6SC03088B

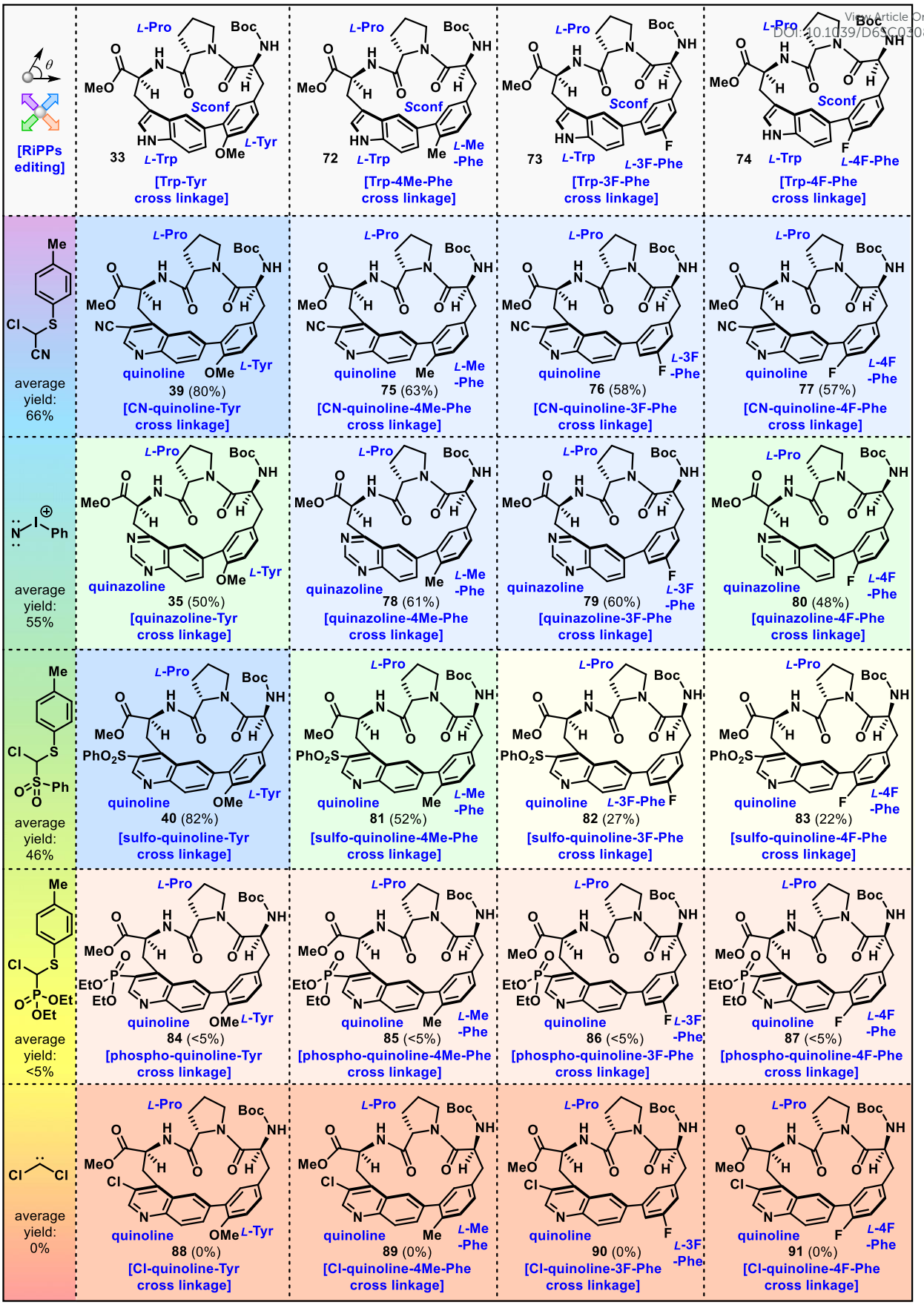

Fig. 5[a] Heat map for the skeletal diversification of the RiPPs core.
[a]For detailed reagents and conditions, see the Supporting Information.

(–CN, –SO_2Ph, –$PO(OEt)_2$), as reported by Sharma and co-workers,[85] together with the nitrene-mediated "*N*–insertion" protocol developed by Morandi and co-workers,[82–84] were applied to RiPP derivatives **33**, **72**-**74**. When a carbene precursor bearing a –CN substituent was employed, skeletal diversification of the RiPPs proceeded rapidly, enabling efficient synthesis of a series of biaryl macrocyclic peptides (**39**, **75**–**77**) incorporating quinoline cores, with an average isolated yield of 66%. Notably, both electron-rich and electron-deficient RiPP scaffolds were competent substrates for this quinoline-forming transformation.

The next most efficient manifold involved nitrene-mediated "*N*–insertion" to construct quinazoline cores. This protocol was successfully applied to all tested RiPP derivatives (**33**, **72**-**74**), providing quinazoline-containing artificial RiPPs **35** and **78**–**80**. As in the quinoline series, both electron-rich and electron-poor RiPPs were tolerated, and the average isolated yield was 55%. In contrast, when carbene precursors bearing a –SO_2Ph substituent were used for skeletal diversification, quinoline derivatives **40** and **81**–**83** were obtained in a somewhat lower average yield of 46%. In this case, electron-deficient RiPP scaffolds (**82**, **83**) tended to give diminished yields, whereas more electron-rich substrates afforded higher yields. In contrast to the case of scabrirubin, no cyclopropane intermediate was observed when the micitide core was employed. On the other hand, for substrates with low yields, although the starting material was completely consumed, multiple unidentified byproducts were obtained. These observations suggest that, in such substrates, cyclopropanation of the indole by the carbene species does proceed, but several undesired side reactions compete simultaneously.

Further studies revealed that the use of carbene precursors bearing a –$PO(OEt)_2$ substituent resulted in almost no formation of quinoline derivatives **84**–**87**; only trace amounts (<5%) were detected for both electron-poor and electron-rich substrates. Finally, as a comparative experiment, classical dichlorocarbene was employed for scaffold hopping of the RiPPs. However, none of the desired products **88**–**91** were obtained, and only decomposition of the substrates was observed. This outcome is plausibly attributable to the rapid generation of dichlorocarbene, which likely leads to a high steady-state carbene concentration in the reaction mixture, thereby promoting overreaction and undesired side processes.

Conclusions

Owing to dramatic advances in genome mining, numerous RiPPs have been discovered in recent years, some of which exhibit potent antibacterial and antitumor activities.[1–6] In the present study, we have developed a general modular synthetic strategy for RiPPs bearing Tyr–Trp cross-linkages, based on C–H arylation. This approach enables gram-scale access to RiPPs that were previously difficult to obtain. Furthermore, we have demonstrated that these RiPPs can undergo skeletal diversification via carbene- and nitrene-mediated transformations to afford artificial biaryl RiPPs incorporating quinazoline–Tyr and quinoline–Tyr cross-linkages, thereby providing systematic access to previously unexplored regions of chemical space. As medium-sized peptides are emerging as a promising modality in drug discovery, the demand for conformationally constrained cyclic peptides with high metabolic stability and strong target protein binding is expected to continue to grow.[132–134] Accordingly, the streamlined synthesis of biaryl-containing RiPPs, together with their skeletal diversification demonstrated herein, is expected to contribute meaningfully toward addressing pressing societal and pharmaceutical demands.

Author contributions

View Article Online
DOI: 10.1039/D6SC03088B

†H. O., Y. L. contributed equally to this work. H. O., Y. L., S. L., T-K. C., and H. N. conducted the experiments. H. N. conceptualized and designed the synthetic strategy. Y. N. conducted the computational study. J. L., Y-X. L. and Y. M. contributed insights into isolation, purification, and structural elucidation. The manuscript was prepared by H. N. with the feedback of all other authors. H. O. and Y. L. prepared the supplementary information under the guidance of H. N.

Conflicts of interest

The authors declare no competing interests.

Data availability

The authors declare that all experimental and computational data generated in this study, including experimental procedures and compound characterization, NMR, and DFT-optimized structure coordinates, are provided in the Supplementary Information. Should any raw data files be needed in another format, they are available from the corresponding author upon request.

Acknowledgements

Financial support for this work was provided by the Research Grants Council of the Hong Kong SAR, China (ECS Project No. 26302024; GRF Project No. 16306525), the National Natural Science Foundation of China (NSFC Project No. NSFC25SC26), and start-up funds from the Hong Kong University of Science and Technology (Project No. R9820) to H.N. This work was partly supported by JSPS KAKENHI Grant Number JP23H03810, JST-ERATO (JPMJER1903), the Institute for Chemical Reaction Design and Discovery (ICReDD), which was established by the World Premier International Research Initiative (WPI), MEXT, Japan (Y.N.), and the Research Enhancement Grant from City University of Hong Kong (Project No. 7020157) to Y.M. The computation was performed using Research Center for Computational Science, Japan (Project: 23-IMS-C119, Y.N.)

References

1 T. Q. N. Nguyen, Y. W. Tooh, R. Sugiyama, T. P. D. Nguyen, M. Purushothaman, L. C. Leow, K. Hanif, R. H. S. Yong, I. Agatha, F. R. Winnerdy, M. Gugger, A. T. Phan and B. I. Morinaka, *Nat. Chem.*, 2020, **12**, 1042–1053.

2 C.-S. Phan and B. I. Morinaka, *Nat. Prod. Rep.*, 2024, **41**, 708–720.

3 M. Zeng, J. Tao, S. Xu, X. Bai and H. Zhang, *Mar. Drugs*, 2023, **21**, 120.

4 A. F. L. Suarez, T. Q. N. Nguyen, L. Chang, Y. W. Tooh, R. H. S. Yong, L. C. Leow, I. Y. F. Koh, H. Chen, J. W. H. Koh, A. Selvanayagam, V. Lim, Y. E. Tan, I. Agatha, F. R. Winnerdy and B. I. Morinaka, *ACS Chem. Biol.*, 2024, **19**, 774–783.

5 H. Nam, J. S. An, J. Lee, Y. Yun, H. Lee, H. Park, Y. Jung, K.-B. Oh, D.-C. Oh and S. Kim, *J. Am. Chem. Soc.*, 2023, **145**, 22047–22057.

6 J. S. An, H. Lee, H. Kim, S. Woo, H. Nam, J. Lee, J. Y. Lee, S.-J. Nam, S. K. Lee, K.-B. Oh, S. Kim and D.-C. Oh, *Angew. Chem. Int. Ed.*, 2023, **62**, e202309139.

7 M. M. Zdouc, J. J. J. van der Hooft and M. H. Medema, *Trends Pharmacol. Sci.*, 2023, **44**, 532–541.
8 H. Li, W. Ding and Q. Zhang, *RSC Chem. Biol.*, 2024, **5**, 90–108.
9 S.-W. Han and H.-S. Won, *Biomolecules*, 2024, **14**, 479.
10 S. Asamizu, *Nat. Prod. Rep.*, 2025, **42**, 1622–1638.
11 K. Pattanayakanahalli Henjarappa, S. Das and N. Mahanta, *Nat. Chem. Biol.*, 2024, **20**, 136–139.
12 R. Liu, C. Pang, G. Wu, B. He, B. Huang, H. Ren, Z. Shen, J. Liu, S. Zhiman, J. Zhou and Y.-X. Li, *bioRxiv*, 2024, DOI: 10.1101/2024.10.06.616194.
13 J. Liu, R. Liu, B.-B. He, X. Lin, L. Guo, G. Wu and Y.-X. Li, *ACS Bio Med Chem Au*, 2024, **4**, 268–279.
14 B. Tan, P. Breunig, L. Arbib, Y. Kakumu, F. Biermann, K. Hardes, J. Hefendehl and E. J. N. Helfrich, *Chem. Sci.*, 2025, **16**, 16240–16249.
15 Y. L. Hu, F. Z. Yin, J. Shi, S. Y. Ma, Z. R. Wang, R. X. Tan, R. H. Jiao and H. M. Ge, *J. Am. Chem. Soc.*, 2023, **145**, 27325–27335.
16 M. Ben-Lulu, E. Gaster, A. Libman and D. Pappo, *Angew. Chem. Int. Ed.*, 2020, **59**, 14722–14726.
17 M. Treisman, L. Coe, Y. Zhao, V. M. Sasi, J. Gullick, M. H. Hansen, A. Ly, V. Leichthammer, C. Hess, D. L. Machell et al., *Org. Lett.*, 2024, **26**, 1828–1833.
18 B.-B. He, J. Liu, Z. Cheng, R. Liu, Z. Zhong, Y. Gao, H. Liu, Z.-M. Song, Y. Tian and Y.-X. Li, *Angew. Chem. Int. Ed.*, 2023, **62**, e202311533.
19 M. T. Bertran, R. Walmsley, T. Cummings, I. V. Aramburu, D. J. Benton, R. Mora Molina, J. Assalaarachchi, M. Chasampalioti, T. Swanton, D. Joshi et al., *Nat. Commun.*, 2024, **15**, 9746.
20 Y. Yang, C. Lee, R. R. Reddy, D. J. Huang, W. Zhong, V. T. B. Nguyen-Tran, W. Shen and Q. Lin, *ACS Chem. Biol.*, 2022, **17**, 1249–1258.
21 J. He, P. Ghosh and C. Nitsche, *Chem. Sci.*, 2024, **15**, 2300–2322.
22 T. Miura, T. R. Malla, L. Brewitz, A. Tumber, E. Salah, K. J. Lee, N. Terasaka, C. D. Owen, C. Strain-Damerell, P. Lukacik et al., *Bull. Chem. Soc. Jpn.*, 2024, **97**, uoae018.
23 L. D. Walensky, A. L. Kung, I. Escher, T. J. Malia, S. Barbuto, R. D. Wright, G. Wagner, G. L. Verdine and S. J. Korsmeyer, *Science*, 2004, **305**, 1466–1470.
24 L. D. Walensky and G. H. Bird, *J. Med. Chem.*, 2014, **57**, 6275–6288.
25 Y. H. Lau, P. de Andrade, Y. Wu and D. R. Spring, *Chem. Soc. Rev.*, 2015, **44**, 91–102.
26 Y. Imai, K. J. Meyer, A. Iinishi, Q. Favre-Godal, R. Green, S. Manuse, M. Caboni, M. Mori, S. Niles, M. Ghiglieri et al., *Nature*, 2019, **576**, 459–464.
27 K. A. Muñoz and P. J. Hergenrother, *Nat. Microbiol.*, 2022, **7**, 1512–1513.
28 J. Schimana, K. Gebhardt, A. Höltzel, D. G. Schmid, R. Süssmuth, J. Müller, R. Pukall and H.-P. Fiedler, *J. Antibiot.*, 2002, **55**, 565–570.
29 I. P.-M. Pfeiffer, M.-P. Schröder and S. Mordhorst, *Nat. Prod. Rep.*, 2024, **41**, 990–1019.
30 W.-J. Wang, X.-M. Dong and G.-B. Li, *Sig. Transduct. Target. Ther.*, 2024, **9**, 81.
31 Y. Zhang, S. Saha, Y. Cheng, Y. C. C. Esser and C. P. Ting, *J. Am. Chem. Soc.*, 2025, **147**, 30661–30673.
32 Y. Zhang, S. Saha, Y. C. C. Esser and C. P. Ting, *J. Am. Chem. Soc.*, 2024, **146**, 17629–17635.
33 H. Nakahara, G. Sennari, H. Azami, H. Tsutsumi, Y. Watanabe, Y. Noguchi, Y. Inahashi, M. Iwatsuki, T. Hirose and T. Sunazuka, *Chem. Sci.*, 2025, **16**, 6060–6069.
34 T. Zhou, M. Katsuragawa, T. Xing, K. Fukaya, T. Okuda, T. Tokiwa, E. Tashiro, M. Imoto, N. Oku, D. Urabe and Y. Igarashi, *J. Nat. Prod.*, 2021, **84**, 327–338.
35 S. M. Rowe and D. R. Spring, *Chem. Soc. Rev.*, 2021, **50**, 4245–4258.
36 D. S. Peters, F. E. Romesberg and P. S. Baran, *J. Am. Chem. Soc.*, 2018, **140**, 2072–2075.
37 J. J. Hug, J. Dastbaz, S. Adam, O. Revermann, J. Koehnke, D. Krug and R. Müller, *ACS Chem. Biol.*, 2020, **15**, 2221–2231.
38 P. Nanudorn, S. Thiengmag, F. Biermann, P. Erkoc, S. D. Dirnberger, T. N. Phan, R. Fürst, R. Ueoka and E. J. N. Helfrich, *Angew. Chem. Int. Ed.*, 2022, **61**, e202208361.
39 C. J. White and A. K. Yudin, *Nat. Chem.*, 2011, **3**, 509–524.
40 J. N. Mitchell and J. P. Roberts, *J. Chem. Soc., Perkin Trans. 1*, 2001, 471–484.
41 J. S. Davies, *J. Pept. Sci.*, 2003, **9**, 471–501.
42 S. Jiang, Z. Li, K. Ding and P. P. Roller, *Curr. Org. Chem.*, 2008, **12**, 1502–1542.
43 R. J. Clark and D. J. Craik, *Biopolymers*, 2010, **94**, 414–422.
44 L. Yu, Y. Nagata and H. Nakamura, *J. Am. Chem. Soc.*, 2024, **146**, 2549–2555.
45 H. Ogawa and H. Nakamura, *Tetrahedron Chem*, 2024, **11**, 100084.
46 J. Zhang, L. Yu, H. Ogawa, Y. Nagata and H. Nakamura, *Angew. Chem. Int. Ed.*, 2024, **63**, e202409987.
47 H. Ogawa, Y. Nagata, T. K. Chan, Y. Matsuda and H. Nakamura, *Angew. Chem. Int. Ed.*, 2025, **64**, e202516053.
48 D. Laws III, E. V. Plouch and S. B. Blakey, *J. Nat. Prod.*, 2022, **85**, 2519–2539.
49 F. Zhu, E. Miller, W. C. Powell, K. Johnson, A. Beggs, G. E. Evenson and M. A. Walczak, *Angew. Chem. Int. Ed.*, 2022, **61**, e202207153.
50 H. Gruß and N. Sewald, *Chem. Eur. J.*, 2020, **26**, 5328–5340.
51 F. Zhu, W. C. Powell, R. Jing and M. A. Walczak, *Chem Catal.*, 2021, **1**, 870–884.
52 Y.-C. Lin, F. Schneider, K. J. Eberle, D. Chiodi, H. Nakamura, S. H. Reisberg, J. Chen, M. Saito and P. S. Baran, *J. Am. Chem. Soc.*, 2022, **144**, 14458–14462.
53 T. C. Roberts, P. A. Smith, R. T. Cirz and F. E. Romesberg, *J. Am. Chem. Soc.*, 2007, **129**, 15830–15838.
54 A. W. Sun, S. Lackner and B. M. Stoltz, *Trends Chem.*, 2019, **1**, 630–643.
55 R. A. Shenvi, *ACS Cent. Sci.*, 2024, **10**, 519–528.
56 B. J. Huffman and R. A. Shenvi, *J. Am. Chem. Soc.*, 2019, **141**, 3332–3346.
57 G. Kang, S. Park and S. Han, *Acc. Chem. Res.*, 2023, **56**, 140–156.
58 T. Huo, X. Zhao, Z. Cheng, J. Wei, M. Zhu, X. Dou and N. Jiao, *Acta Pharm. Sin. B*, 2024, **14**, 1030–1076.
59 C. Ma, C. W. Lindsley, J. Chang and B. Yu, *J. Med. Chem.*, 2024, **67**, 11459–11466.
60 Y. Ji, Y. Liu, W. Guan, C. Guo, H. Jia, B. Hong and H. Li, *J. Am. Chem. Soc.*, 2024, **146**, 9395–9403.
61 G. Huang, X. Zhang, Y.-C. Gu and J. Gui, *J. Am. Chem. Soc.*, 2025, **147**, 20239–20245.
62 C. Chen, Y. Yin, P. Lu, T. Han, H. Wang and C. Li, *Angew. Chem. Int. Ed.*, 2025, **64**, e202415439.
63 S. Kawano, N. Miyamoto, K. Fujioka, H. Toya, J. Sakata and H. Tokuyama, *Angew. Chem. Int. Ed.*, 2025, **64**, e21481.
64 H. Nakahara, T. Okano, G. Sennari, M. Iwatsuki, T. Sunazuka and T. Hirose, *JACS Au*, 2025, **5**, 5932–5938.
65 B. D. A. Shennan, T. Fukuta, M. Yamane, T. Koyama, H. Mitsunuma and M. Kanai, *J. Am. Chem. Soc.*, 2025, **147**, 6349–6354.
66 J. Ni, T. Oguro, T. Sawazaki, Y. Sohma and M. Kanai, *Org. Lett.*, 2018, **20**, 7371–7374.
67 R. Sharma, M. Arisawa, S. Takizawa and M. S. H. Salem, *Org. Chem. Front.*, 2025, **12**, 1633–1670.
68 B. W. Joynson and L. T. Ball, *Helv. Chim. Acta*, 2023, **106**, e202200182.

69 C. Hui, Z. Wang, S. Wang and C. Xu, *Org. Chem. Front.*, 2022, **9**, 1451–1457.
70 E.-Q. Li, C. W. Lindsley, J. Chang and B. Yu, *J. Med. Chem.*, 2024, **67**, 13509–13511.
71 R. Al-Ahmad and M. Dai, *Acc. Chem. Res.*, 2025, **58**, 1392–1406.
72 B. D. Dherange, P. Q. Kelly, J. P. Liles, M. S. Sigman and M. D. Levin, *J. Am. Chem. Soc.*, 2021, **143**, 11337–11344.
73 S. Liu, Y. Yang, Q. Song, Z. Liu, Y. Lu, Z. Wang, P. Sivaguru and X. Bi, *Nat. Chem.*, 2024, **16**, 988–997.
74 S. Tsuchiya, H. Saito, K. Nogi and H. Yorimitsu, *Org. Lett.*, 2019, **21**, 3855–3860.
75 Z. Wang, P. Xu, S.-M. Guo, C. G. Daniliuc and A. Studer, *Nature*, 2025, **642**, 92–98.
76 H.-H. Li, Y. Xiao, H. Liu and X. Li, *J. Am. Chem. Soc.*, 2025, **147**, 35211–35218.
77 X.-Y. Huang, P.-P. Xie, L.-M. Zou, C. Zheng and S.-L. You, *J. Am. Chem. Soc.*, 2023, **145**, 11745–11753.
78 D. Kim, J. You, D. H. Lee, H. Hong, D. Kim and Y. Park, *Science*, 2024, **386**, 99–105.
79 G.-Q. Sun, X. Wang, R. Hu, W. Rao, Y. Zhao and M. J. Koh, *Nat. Synth.*, 2025, **4**, 466–475.
80 Y.-Q. Zhang, S.-H. Li, X. Zhang and M. J. Koh, *Nature*, 2025, **647**, 906–912.
81 H. Ogawa, Y. Nagata and H. Nakamura, *Chin. J. Chem.*, 2024, **42**, 2845–2852.
82 J. C. Reisenbauer, O. Green, A. Franchino, P. Finkelstein and B. Morandi, *Science*, 2022, **377**, 1104–1109.
83 A.-S. K. Paschke, E. J. Meeus, M. A. Masota, F. Hoffmann, N. M. Grob and B. Morandi, *J. Am. Chem. Soc.*, 2025, **147**, 1120–1132.
84 J. C. Reisenbauer, A.-S. K. Paschke, J. Krizic, B. B. Botlik, P. Finkelstein and B. Morandi, *Org. Lett.*, 2023, **25**, 8419–8423.
85 P. Kafle, D. Herndon and I. Sharma, *J. Am. Chem. Soc.*, 2025, **147**, 13824–13832.
86 P. Kafle, P. Kharel, D. Nilson, S. Yasuda and I. Sharma, *ChemRxiv*, 2025, DOI: 10.26434/chemrxiv-2025-vkfzx.
87 A. F. M. Noisier and M. Brimble, *Chem. Rev.*, 2014, **114**, 8775–8806.
88 Q. Shao, K. Wu, Z. Zhuang, S. Qian and J.-Q. Yu, *Acc. Chem. Res.*, 2020, **53**, 833–851.
89 G. He, B. Wang, W. A. Nack and G. Chen, *Acc. Chem. Res.*, 2016, **49**, 635–645.
90 O. Daugulis, H.-Q. Do and D. Shabashov, *Acc. Chem. Res.*, 2009, **42**, 1074–1086.
91 H. M. L. Davies, J. Bois and J.-Q. Yu, *Chem. Soc. Rev.*, 2011, **40**, 1855–1856.
92 D. Y.-K. Chen and S. W. Youn, *Chem. Eur. J.*, 2012, **18**, 9452–9474.
93 H. Zhai, K. Lv, J. Li, J. Wang, T. Liu and C. Zhao, *J. Am. Chem. Soc.*, 2024, **146**, 29214–29223.
94 J. Li, Z. Dong, C. Yuan and C. Zhao, *CCS Chem.*, 2024, **6**, 1245–1257.
95 Y. Zhu, X. Chen, C. Yuan, G. Li, J. Zhang and Y. Zhao, *Nat. Commun.*, 2017, **8**, 14904.
96 Q. Zhang, K. Chen, W. Rao, Y. Zhang, F.-J. Chen and B.-F. Shi, *Angew. Chem. Int. Ed.*, 2013, **52**, 13588–13592.
97 S. Aspin, A.-S. Goutierre, P. Larini, R. Jazzar and O. Baudoin, *Angew. Chem. Int. Ed.*, 2012, **51**, 10808–10811.
98 G. Chen, T. Shigenari, P. Jain, Z. Zhang, Z. Jin, J. He, S. Li, C. Mapelli, M. M. Miller, M. A. Poss et al., *J. Am. Chem. Soc.*, 2015, **137**, 3338–3351.
99 G. Chen, Z. Zhuang, G.-C. Li, T. G. Saint-Denis, Y. Hsiao, C. L. Joe and J.-Q. Yu, *Angew. Chem. Int. Ed.*, 2017, **56**, 1506–1509.
100 J. He, S. Li, Y. Deng, H. Fu, B. N. Laforteza, J. E. Spangler, A. Homs and J.-Q. Yu, *Science*, 2014, **343**, 1216–1220.
101 M. Guan, Y. Pang, J. Zhang and Y. Zhao, *Chem. Commun.*, 2016, **52**, 7043–7046.
102 X. Li, L. Qi, B. Li, Z. Zhao, G. He and G. Chen, *Org. Lett.*, 2020, **22**, 6209–6213.
103 K. Chen, F. Hu, S.-Q. Zhang and B.-F. Shi, *Chem. Sci.*, 2013, **4**, 3906–3911.
104 Y. Feng and G. Chen, *Angew. Chem. Int. Ed.*, 2010, **49**, 958–961.
105 B. Wang, W. A. Nack, G. He, S.-Y. Zhang and G. Chen, *Chem. Sci.*, 2014, **5**, 3952–3957.
106 L. D. Tran and O. Daugulis, *Angew. Chem. Int. Ed.*, 2012, **51**, 5188–5191.
107 S.-Y. Zhang, Q. Li, G. He, W. A. Nack and G. Chen, *J. Am. Chem. Soc.*, 2013, **135**, 12135–12141.
108 M. Berger, R. Chauhan, C. A. B. Rodrigues and N. Maulide, *Chem. Eur. J.*, 2016, **22**, 16805–16808.
109 H. Wang, Z. Bai, T. Jiao, Z. Deng, H. Tong, G. He, Q. Peng and G. Chen, *J. Am. Chem. Soc.*, 2018, **140**, 3542–3546.
110 Z. Zhang, X. Li, M. Song, Y. Wan, D. Zheng, G. Zhang and G. Chen, *J. Org. Chem.*, 2019, **84**, 12792–12799.
111 G. He, S.-Y. Zhang, W. A. Nack, Q. Li and G. Chen, *Angew. Chem. Int. Ed.*, 2013, **52**, 11124–11128.
112 D. Shabashov and O. Daugulis, *J. Am. Chem. Soc.*, 2010, **132**, 3965–3972.
113 K. R. Holman, A. M. Stanko and S. E. Reisman, *Chem. Soc. Rev.*, 2021, **50**, 7891–7908.
114 L. Li, Q. Yang, Y. Wang and Y. Jia, *Angew. Chem. Int. Ed.*, 2015, **54**, 6255–6259.
115 H. Liu, X. Zhang, D. Shan, M. Pitchakuntla, Y. Ma and Y. Jia, *Org. Lett.*, 2017, **19**, 3323–3326.
116 D. Shan, Y. Gao and Y. Jia, *Angew. Chem. Int. Ed.*, 2013, **52**, 4902–4905.
117 K. V. Chuang, M. E. Kieffer and S. E. Reisman, *Org. Lett.*, 2016, **18**, 4750–4753.
118 F. Schneider, Y. Guo, Y.-C. Lin, K. J. Eberle, D. Chiodi, J. A. Greene, C. Lu and P. S. Baran, *J. Am. Chem. Soc.*, 2024, **146**, 6444–6448.
119 M. Nesic, D. B. Ryffel, J. Maturano, M. Shevlin, S. R. Pollack, D. R. Gauthier Jr., P. Trigo-Mouriño et al., *J. Am. Chem. Soc.*, 2022, **144**, 14026–14030.
120 N. A. Isley, Y. Endo, Z.-C. Wu, B. C. Covington, L. B. Bushin, M. R. Seyedsayamdost and D. L. Boger, *J. Am. Chem. Soc.*, 2019, **141**, 17361–17369.
121 S. P. Breazzano, Y. B. Poudel and D. L. Boger, *J. Am. Chem. Soc.*, 2013, **135**, 1600–1606.
122 J. Garfunkle, F. S. Kimball, J. D. Trzupek, S. Takizawa, H. Shimamura, M. Tomishima and D. L. Boger, *J. Am. Chem. Soc.*, 2009, **131**, 16036–16038.
123 T. Newhouse, C. A. Lewis and P. S. Baran, *J. Am. Chem. Soc.*, 2009, **131**, 6360–6361.
124 M. E. Kieffer, K. V. Chuang and S. E. Reisman, *J. Am. Chem. Soc.*, 2013, **135**, 5557–5560.
125 B. Fu, C. Li, L. Bai and X. Jiang, *Angew. Chem. Int. Ed.*, 2026, **65**, e21607.
126 C. Schöneich, *J. Pharm. Pharmacol.*, 2018, **70**, 655–665.
127 S. Bellmaine, A. Schnellbaecher and A. Zimmer, *Free Radic. Biol. Med.*, 2020, **160**, 696–718.
128 S. R. Laplante, L. D. Fader, K. R. Fandrick, D. R. Fandrick, O. Hucke, R. Kemper, S. P. F. Miller and P. J. Edwards, *J. Med. Chem.*, 2011, **54**, 7005–7022.
129 S. Swallow, *Prog. Med. Chem.*, 2015, **54**, 65–133.
130 G. Shabir, A. Saeed, W. Zahid, F. Naseer, Z. Riaz, N. Khalil, Muneeba and F. Albericio, *Pharmaceuticals*, 2023, **16**, 1162.
131 E. P. Gillis, K. J. Eastman, M. D. Hill, D. J. Donnelly and N. A. Meanwell, *J. Med. Chem.*, 2015, **58**, 8315–8359.
132 X. Ji, A. L. Nielsen and C. Heinis, *Angew. Chem. Int. Ed.*, 2024, **63**, e202308251.

View Article Online
DOI: 10.1039/D6SC03088B

133 L. Wang, N. Wang, W. Zhang, X. Cheng, Z. Yan, G. Shao, X. Wang, R. Wang and C. Fu, *Sig. Transduct. Target. Ther.*, 2022, **7**, 48.
134 D. Sharma, I. Dhiman, S. Das, D. K. Das, D. D. Pramanik, S. K. Dash and A. Pramanik, *ACS Omega*, 2025, **10**, 17087–17107.

View Article Online
DOI: 10.1039/D6SC03088B

Data Availability Statement

The authors declare that the data supporting the findings of this study are available within the article and the supplementary information (SI) as well as from the authors upon request. Supplementary information: experimental procedures, experimental equipment, characterization data, computational results, HRMS, and NMR spectra for all new compounds.